DNS and LES of scalar transport in a turbulent plane channel flow at low Reynolds number

Jordan A. Denev[1], Jochen Fröhlich[1], Henning Bockhorn[1],
Florian Schwertfirm[2], Michael Manhart[2]

[1] Institute for Technical Chemistry and Polymer Chemistry, University of Karlsruhe,
Kaiserstraße 12, D-76128 Karlsruhe, Germany,
denev@ict.uni-karlsruhe.de, http://www.ict.uni-karlsruhe.de
[2] Department of Hydromechanics, Technical University of Munich,
Arcisstraße 21, 80333 Munich, Germany

Abstract. The paper reports on DNS and LES of plane channel flow at $Re_\tau = 180$ and compares these to a DNS with a higher order convection scheme. For LES different subgrid-scale models like the Smagorinsky, the Dynamic Smagorinsky and the Dynamic Mixed Model were used with the grid being locally refined in the near-wall region. The mixing of a passive scalar has been simulated with two convection schemes, central differencing and $HLPA$. The latter exhibits numerical diffusion and the results with the central scheme are clearly superior. LES with this scheme reproduced the budget of the scalar variance equation reasonably well.

1 Introduction

Turbulent mixing of scalar quantities is a phenomenon observed in environmental flows as well as in abundant engineering applications of chemical, nuclear power, pharmaceutical or food industries. Their simulation requires reliable models for turbulent mixing processes. After discretization, however, the physical and the numerical model interact in a complex way, which is not fully understood so far. To address these issues, this paper presents results from both, Direct Numerical Simulations (DNS) and Large Eddy Simulations (LES) of fully developed plane channel flow at a friction Reynolds number of $Re_\tau = 180$. This is a prototypical flow frequently used to study physical and numerical modelling of wall-bounded flows. The first DNS of this configuration was performed by Kim *et al.* [4].

In an earlier paper by the present authors [2] the impact of local grid refinement near the walls on the LES modelling of the flow field was investigated. In the present paper we extend this approach and focus on the modelling of a transported scalar.

2 Numerical methods and simulation details

The turbulent channel flow between two parallel plates is simulated for a nominal friction Reynolds number $Re_\tau = 180$, defined by the friction velocity U_τ and the

channel half-width h. In the computation, the corresponding bulk Reynolds number $Re_b = 2817$ was imposed by instantaneously adjusting a spatially constant volume force in each time step, so that in fact U_τ and hence Re_τ is a result of the simulation. The computational domain in streamwise, wall-normal and spanwise direction extends over $L_x = 6.4h$, $L_y = 2.0h$ and $L_z = 3.2h$, respectively. Periodic boundary conditions were imposed for the streamwise and the spanwise direction. At the walls, a no-slip condition was applied for both LES and DNS, together with Van Driest damping for the Smagorinsky model. Dirichlet boundary conditions at the walls were imposed for the scalar, i.e. $C(x, 0, z) = 1.0$ and $C(x, 2h, z) = -1.0$.

Two different numerical codes have been applied for the present work. Both utilize a finite volume method for incompressible fluid on block-structured grids together with a Runge-Kutta (RK) scheme in time. A Poisson equation is solved for the pressure-correction. The code $MGLET$ has been developed at the TU Munich and uses staggered Cartesian grids with a 6th order central discretization scheme (CDS) in space and a 3rd order RK scheme [5, 8]. The code $LESOCC2$, developed at the University of Karlsruhe, can handle curvilinear collocated grids and employs discretizations of second order in space and time [3]. In the present study, DNS results from this code were first compared to those obtained with the higher-order discretization of $MGLET$. Subsequently, LES were carried out with different subgrid-scale (SGS) models as described, e.g., in [6]. These comprise the Smagorinsky Model (SM) with constant $C_S = 0.1$, the Dynamic Smagorinsky Model (DSM), and the Dynamic Mixed Model (DMM), see Table 1. The first case in Table 1, denoted $DNS-6O$ (sixth order discretization in space for both convection and diffusion), has been calculated with $MGLET$, all others with $LESOCC2$. The LES filter is not accounted for in the present notation.

An equation governing the transport of a scalar quantity with Schmidt number $Sc = 1$ is also considered in the present study. The concentration C, is regarded as passive, i.e. it does not influence the fluid flow. The unresolved turbulent transport of C is modelled by an eddy diffusivity $D_t = \nu_t/Sc_t$, where ν_t is the SGS eddy viscosity and Sc_t the turbulent Schmidt number, here set equal to 0.6. This also holds for the mixed model.

With the present equations and Dirichlet boundary conditions the concentration fulfils a maximum condition. The extrema are attained on the boundaries, so that the scalar is restricted to the interval $C \in [-1; 1]$ for physical reasons (the lower bound -1 was chosen here instead of 0 for technical reasons). This boundedness does not neccessarily carry over to the discretized solution. In numerous studies bounded convection schemes are therefore applied to guarantee the boundedness of the numerical solution which is not guaranteed with a central scheme. In [3] and related work the $HLPA$ scheme developed in [9] was used for this purpose. $HLPA$ determines the convective flux by a blending between second-order upwinding and first-order upwinding as

$$F_{i+\frac{1}{2}} = \begin{cases} UC_i + U(C_{i+1} - C_i)\Theta_{i+\frac{1}{2}} & , 0 < \Theta_{i+\frac{1}{2}} < 1 \\ UC_i & , \text{else} \end{cases} , \; \Theta_{i+\frac{1}{2}} = \frac{C_i - C_{i-1}}{C_{i+1} - C_{i-1}} , \quad (1)$$

where U is the velocity at the cell boundary $i+1/2$. This scheme was employed for the present study for the convection term of the concentration equation in cases DNS and $DNS-F$, while still using second order CDS in the momentum equation (see the column for the scalar convection scheme (SCS) in Table 1).

Table 1. Overview over the runs discussed. The nomenclaure is defined in the text.

Case	CV_{tot}	Δ_x^+	y_1^+	Δ_z^+	SGS	SCS	t_{av}	U_τ	C_τ
DNS									
DNS-6O	1,407,120	9.1	0.68	7.2	-	CDS-6O	544	0.064018	-0.041478
DNS	1,407,120	9.1	0.68	7.2	-	HLPA	638	0.062237	-0.039232
DNS-F	10,866,960	4.5	0.34	3.6	-	HLPA	537	0.061821	-0.041106
DNS-CDS	1,407,120	9.1	0.68	7.2	-	CDS	745	0.062487	-0.042083
LES									
HLPA-SM	258,688	29.8	0.37	14.9	SM	HLPA	615	0.067434	-0.038431
CDS-SM	258,688	29.8	0.37	14.9	SM	CDS	643	0.066032	-0.047632
CDS-DSM	258,688	29.8	0.37	14.9	DSM	CDS	650	0.060801	-0.042553
CDS-DMM	258,688	29.8	0.37	14.9	DMM	CDS	646	0.070095	-0.043067

A special feature of the code $LESOOC2$ is the possibility of block-wise local grid refinement (LGR). This allows to use a fine grid close to the walls without excessively refining in the center of the channel, so that CPU time and storage are not overly increased. LGR is utilized near the walls up to a distance $y_{ref} = h/8$ equal to $y_{ref}^+ = 22.5$ from the wall with a refinement ratio of 2 in both, $x-$ and $z-$direction. In $y-$direction the grid is stretched uniformly by a factor 1.03 throughout the channel. As observed in a previous study [2] the turbulent characteristics of the flow exhibit some visible changes at the block-interface, and this issue will also be addressed later in this paper. Table 1 presents information on the numerical grids, i.e. the total number of control volumes of the entire grid, CV_{tot}, and the dimensionless size of the control volumes in $x-$ and $z-$direction, respectively. In case of LGR, which is used with all LES cases, this is the unrefined spacing used in the core of the flow. Furthermore, y_1^+ indicates the distance of the wall-adjacent point from the wall.

3 Results from DNS

Statistical data for all computations in the present work have been collected over averaging times t_{av} larger than 540 dimensionless time units $t_b = h/U_b$, where U_b is the bulk velocity of the flow. Table 1 shows the results obtained for the friction velocity and the reference concentration defined as

$$U_\tau = \sqrt{\frac{\tau_w}{\rho}} \qquad , \qquad C_\tau = \frac{D}{U_\tau}\left(\frac{\partial\langle C\rangle}{\partial y}\right)_{y=0}, \tag{2}$$

respectively, with D being the laminar diffusion coefficient (the turbulent diffusion coefficient vanishes at the wall). In the present section four DNS cases are compared, which allows to identify the role of the numerical discretization scheme and the grid resolution. Case $DNS-6O$ is chosen as a reference case. In [7] these data were compared with the classical ones of [4] showing excellent agreement. The run DNS was performed with $LESOCC2$ on the collocated equivalent of this grid with the second order method. Due to the lower order these results (not reproduced here) were unsatisfactory showing deviations of up to 18% from the reference data. Therefore, the grid was refined by a factor of 2 in each direction (case $DNS-F$) to compensate for the lower-order discretization. The comparison with $DNS-6O$ is presented in Figure 1. The turbulent stresses and the time-averaged scalar match very well. The turbulent scalar flux $\langle u'c'\rangle$ and the scalar variance $\langle c'c'\rangle$ exhibit differences, which for the latter mainly appear in the middle of the channel.

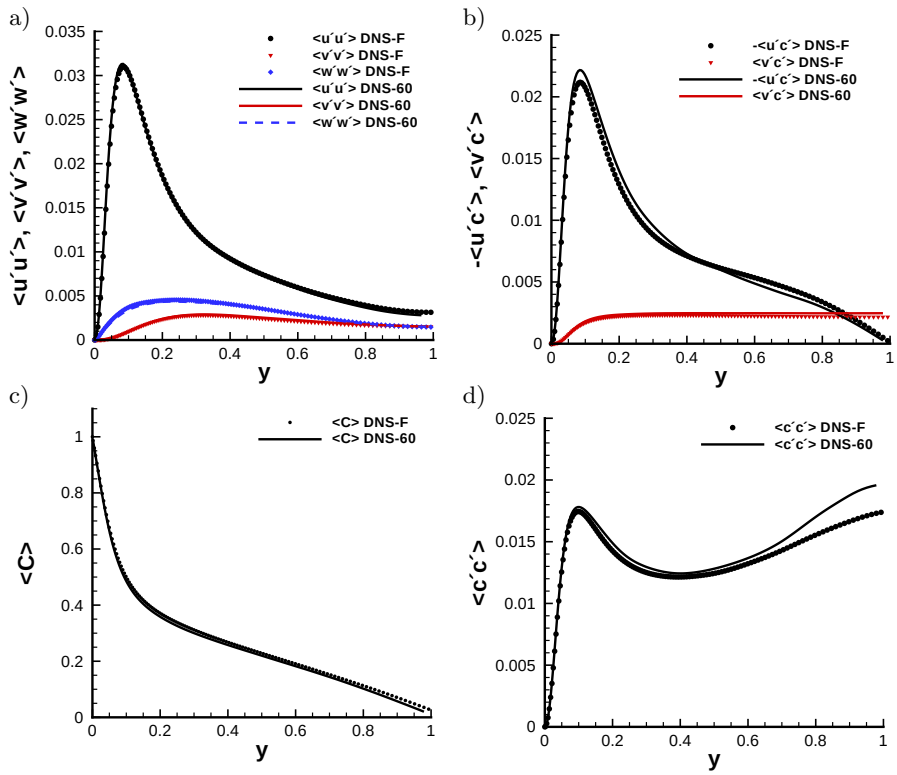

Fig. 1. Comparison of the results from cases $DNS-6O$ and $DNS-F$: a) normal turbulent stresses $\langle u'u'\rangle$, $\langle v'v'\rangle$ and $\langle w'w'\rangle$; b) turbulent scalar fluxes $\langle u'c'\rangle$ and $\langle v'c'\rangle$; c) mean scalar $\langle C\rangle$; d) scalar variance $\langle c'c'\rangle$.

In order to further elucidate the role of the numerical scheme, case DNS has been repeated employing the CDS scheme of second order instead of the $HLPA$ scheme. These results (not depicted here for lack of space) show a clear improvement for the scalar variance $\langle c'c' \rangle$ compared to case DNS, and also when compared to case $DNS-F$, as the difference with respect to the reference data in the middle of the channel decreases. The scalar flux $\langle v'c' \rangle$ for $DNS-CDS$ matches perfectly well with $DNS-6O$ and the agreement of $\langle u'c' \rangle$ is practically as good as for $DNS-F$ in Figure 1. It should also be noticed that the value for the reference scalar C_τ for this case is closer to the value of $DNS-6O$ than that of DNS. This considerable improvement from case DNS to $DNS-CDS$ shows that for the flow considered the central differencing scheme appears clearly superior compared to the $HLPA$ scheme.

4 Results from LES

The results of the previous section were obtained with DNS, i.e. on fine grids and without any turbulence model. Now we turn to LES for which numerical and modelling errors interact in a complex way. The grid used for these LES is much coarser in the core region of the flow (see Δx^+ and Δz^+ in Table 1), while in the vicinity of the wall ($y < 1/8h$) it is of similar cell size as in the DNS cases (195,000 control volumes in the region of refinement).

The results obtained with the CDS for the convective terms of the scalar transport equation confirm the findings of a previous paper by the authors [2], in which a higher Reynolds number was considered, and where the Smagorinsky model performed better than the other two models. In the present investigation, $CDS-DMM$ shows slightly better results than $CDS-DSM$. This assertion is mainly based on the behaviour of the averaged scalar and the scalar variance near the wall. $CDS-DSM$ on the other hand shows the most accurate LES value for C_τ.

To address the impact of the convection scheme, results for the cases $CDS-SM$ and $HLPA-SM$ are presented together with the reference case $DNS-6O$ in Figure 2. These results again show the superiority of the CDS, which is more pronounced in the proximity of the wall. The results also demonstrate the diffusive characteristics of the $HLPA$ scheme. The presence of additional diffusion is noticed in the averaged scalar distribution by an increased value and an almost linear distribution for the region away from the wall. Furthermore, the turbulence quantities such as the scalar fluxes and the scalar variance are underestimated near the wall, i.e. damped by the numerical diffusion.

5 Transport equation of the scalar variance

Finally, an evaluation of the terms in the budget of the scalar variance was carried out. In the case of the Smagorinsky model the equation for the resolved

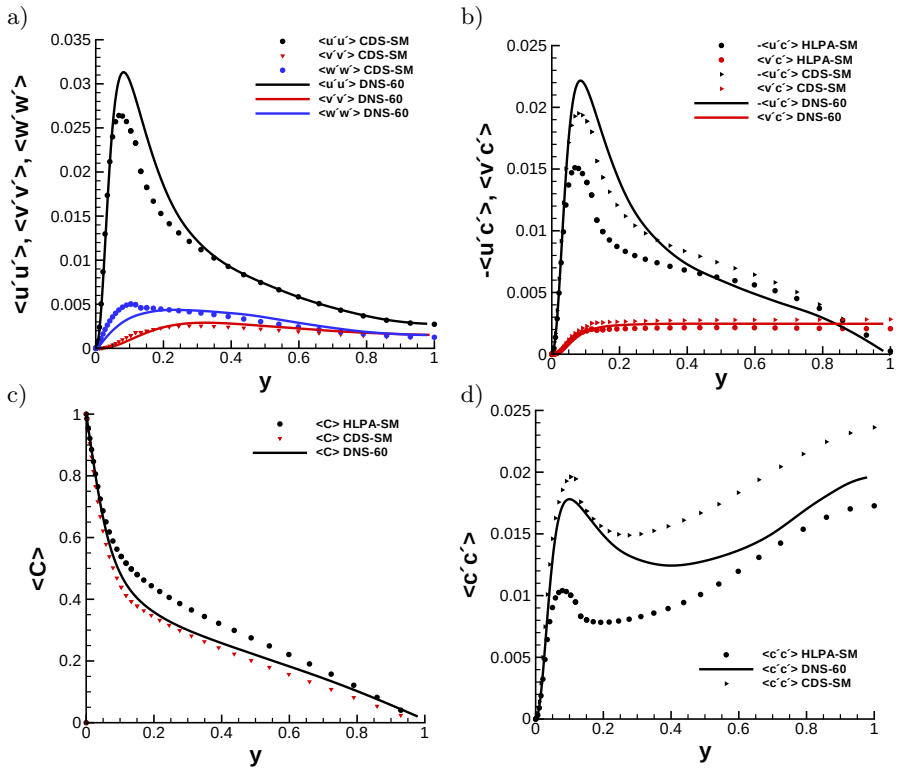

Fig. 2. Computations performed with LES and different numerical schemes for the scalar: cases $CDS-SM$ and $HLPA-SM$ compared with the reference case $DNS-6O$. a),b),c) and d) as in the previous figure.

scalar variance reads

$$0 = \underbrace{-2\langle c'v'\rangle\frac{\partial\langle C\rangle}{\partial y}}_{P_C} \underbrace{-2\left\langle (D+D_t)\left(\frac{\partial c'}{\partial x_k}\right)^2\right\rangle}_{E_C} + \underbrace{\frac{\partial}{\partial y}\left(\langle D+D_t\rangle\frac{\partial\langle c'\rangle^2}{\partial y}\right)}_{D_C} \underbrace{-\frac{\partial}{\partial y}(\langle c'^2v'\rangle)}_{T_C}$$

Here, Pc denotes the production by the mean concentration gradients, Ec the scalar dissipation, Dc the diffusion transport term (comprises molecular and, in the case of LES, eddy-diffusion) and Tc turbulent transport by the normal velocity fluctuation. In the case of dynamic LES-models, additional terms appear in the balance due to the fluctuation of the model parameter. These are however negligible compared to the other terms of the equation [1]. In the case of DNS the tubulent diffusivity is omitted.

Figure 3 shows the comparison of the different terms, constituting the budget of the scalar variance for $DNS-6O$, $DNS-CDS$ and $CDS-SM$. While for the first two cases the match is very good, the case $CDS-SM$ shows some differences. As expected, the magnitude of the terms in the middle of the

channel is underestimated, which is due to the fact that only part of the turbulent spectrum is resolved with LES. The values at the wall on the other hand are quite accurately reproduced for all terms of the above equation due to the fine grid near the walls. For $CDS-SM$ the Figure 3b shows some artefacts at the block boundary separating the refined and the coarse grid. They are present only in those terms containing a derivative of a correlation term normal to the wall, i.e. in Ec, Dc and Tc. The reason is that the abrupt changes in the subgrid-filter size and the numerical resolution cause inevitable irregularities in the turbulent quantities at the two sides of the block boundary which modify the derivative operator applied normal to the wall. Apart from this, the agreement between the $CDS-SM$ and the DNS cases is reasonably good. It can hence be concluded that in the present case LES (case $CDS-SM$) is capable of qualitatively, and to some extent also quantitatively, reproducing the terms in the budget for the scalar variance.

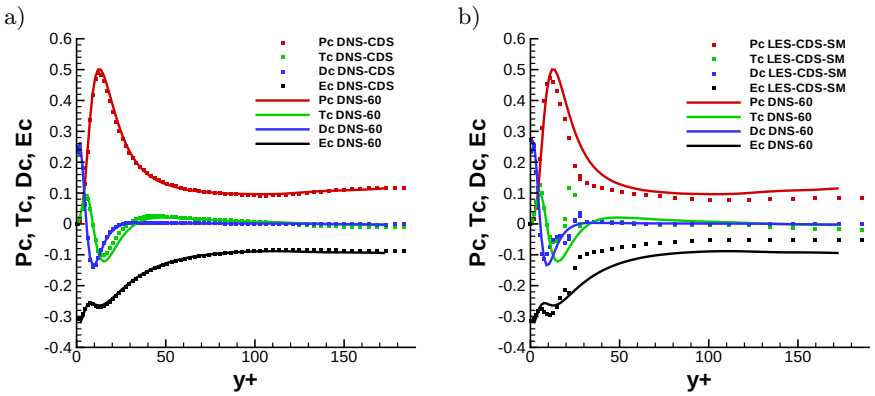

Fig. 3. Terms in the budget of the scalar variance $\langle c'c' \rangle$. All terms are normalized by $D/(C_\tau^2 U_\tau^2)$ and explained in the text. a) Case $DNS-CDS$ (symbols) compared to reference case $DNS-6O$ (lines). b) LES with $CDS-SM$ (symbols) compared to $DNS-6O$ (lines).

6 Conclusions

Different numerical and modeling issues have been studied when calculating fluid flow and passive scalar distribution in a plane turbulent channel flow. DNS with CDS of sixth and second order accuracy have been compared. It has been shown, that the second-odrer scheme achieved the desired accuracy (shown by the sixth-order CDS) only after the numerical grid has been refined twice in each spatial direction.

Comparison of two schemes for the scalar, unbounded CDS and non-linear, monotonous upstream-weighted $HLPA$ showed superiority of the CDS scheme,

while the results with $HLPA$ were found to suffer from numerical diffusion. This is in line with the general attitude when modelling the SGS terms in the LES-momentum equation. Usually, a non-dissipative scheme is preferred and dissipation entirely introduced by the laminar viscous terms and the SGS model. Additional numerical dissipation without modifying the SGS model is avoided. The same is observed here for the scalar transport. It should however not be concluded that the CDS is best for any LES involving a passive scalar. In other simulations of the present authors concerned with a jet in crossflow this scheme led to numerical instability. More appropriate schemes to maintain boundedness of the scalar are needed.

The present study shows that LES with tangential grid refinement near the walls delivers reasonable accuracy at low computational costs. This conclusion is also supported by the results obtained for the budget of the scalar variance which is reproduced reasonably well with the present LES.

Acknowledgements: This research was funded by the German Research foundation through priority programme SPP-1141 "Mixing devices". Carlos Falconi helped with the preparation of figures.

References

1. I. Calmet and J. Magnaudet. Large-eddy simulation of high-schmidt number mass transfer in a turbulent channel flow. *Phys. Fluids*, 9(2):438–455, 1997.
2. J. Fröhlich, J. A. Denev, C. Hinterberger, and H. Bockhorn. On the impact of tangential grid refinement on subgrid-scale modeling in large eddy simulation. In T. Boyanov et al., editor, *Numerical methods and applications, 6th International conference NMA 2006*, LNCS 4310, pages 550–557, Borovets, Bulgaria, August 2006. Springer-Verlag Berlin Heidelberg 2007.
3. C. Hinterberger. *Dreidimensionale und tiefengemittelte Large–Eddy–Simulation von Flachwasserströmungen*. PhD thesis, Institute for Hydromechanics, University of Karlsruhe, 2004.
4. J. Kim, P. Moin, and R. Moser. Turbulence statistics in fully developed channel flow at low Reynolds number. *J. Fluid Mech.*, 177:133–166, 1987.
5. M. Manhart. Large-eddy simulation of high-schmidt number mass transfer in a turbulent channel flow. *Computers and Fluids*, 33(3):435–461, March.
6. P. Sagaut. *Large Eddy Simulation for Incompressible Flows: An Introduction, second ed.* Springer, Berlin, Oktober 2002.
7. F. Schwertfirm and M. Manhart. ADM Modelling for Semi-Direct Numerical Simulation of Turbulent Mixing and Mass Transport. In J.A.C. Humphrey, T.B. Gatski, J.K. Eaton, R. Friedrich, N. Kasagi, and M.A. Leschziner, editors, *Fourth International Symposium. on Turbulence and Shear Flow Phenomena*, volume 2, pages 823–828, Williamsburg, Virginia, 2005.
8. F. Schwertfirm and M. Manhart. DNS of passive scalar transport in turbulent channel flow at high Schmidt numbers. In K. Hanjalic, Y. Nagano, and S. Jakrilic, editors, *Turbulence, Heat and Mass Transfer 5*, pages 289–292, Dubrovnik, Coratia, 2006.
9. J. Zhu. A low-diffusive and oscillation-free convection scheme. *Communications in applied numerical methods*, 7:225–232, 1991.